

# Numerical simulation of damping effects on free-surface motions due to deformable bodies

Satoru Ushijima<sup>1,\*</sup>, Niku Guinea<sup>2</sup>, Daisuke Toriu<sup>1</sup>, Atomu Kuki<sup>3</sup>

<sup>1</sup>Academic Center for Computing and Media Studies (ACCMS), Kyoto University

<sup>2</sup>Research Student, ACCMS, Kyoto University

<sup>3</sup>Faculty of Engineering, Kyoto University

\*ushijima.satoru.3c@kyoto-u.ac.jp

**Abstract.** The damping effects on the free-surface motions due to the presence of the deformable solid bodies suspended in the fluid were numerically investigated. The computational method is based on the Eulerian method that can deal with the interactions between the Newtonian fluids and visco-hyperelastic solid bodies. In the numerical experiments, the free-surface motions caused by the so-called dam-break conditions, including four spherical visco-hyperelastic bodies, were calculated with two cases of non-dimensional shear moduli,  $G = 0.1$  and  $10.0$ , of the visco-hyperelastic bodies, which have the same density as that of the fluid. As a result of the computations, the following reasonable results were obtained: when the solid bodies are sufficiently flexible ( $G = 0.1$ ), the free-surface motions are almost same as those having no solid bodies. In contrast, it was demonstrated that the damping effects are obviously large in case that the solid bodies are relatively rigid ( $G = 10.0$ ).

**Keywords:** Free-surface motion, visco-hyperelastic model, Eulerian method

## 1. Introduction

It is known that the free-surface motions are affected by the solid objects suspended in the fluid. In case that the solid objects are made of deformable material and their density is same as that of the fluid, it is expected that the effects on the free-surface motions increase as the stiffness of the material increases.

The purpose of this study is to demonstrate such tendency can be numerically predicted with a suitable computational method. We adopt partial differential equations for left Cauchy-Green deformation tensor of hyperelastic solid objects [1], [2]. Taking account of the viscosity, the partial differential equations are solved with Navier-Stokes equations to deal with the interactions between Newtonian fluids and visco-hyperelastic solid objects. In this method, all governing equations are discretized with a finite volume method (FVM) on the collocated Eulerian grid system fixed in the space.

In this study, the dam-break flows including spherical visco-hyperelastic bodies were calculated to investigate the damping effects of the stiffness in the suspended objects on

free-surface motions. Thus, two cases of computations were conducted with  $G = 0.1$  and  $10.0$ . As a result of the computations, the following reasonable results were obtained: it was confirmed that the free-surface motions are almost same as those having no solid bodies when the visco-hyperelastic bodies are sufficiently flexible ( $G = 0.1$ ), while the damping effects are obviously large in case that the solid bodies are relatively rigid ( $G = 10.0$ ).

## 2. Numerical methods

The phase-averaged governing equations are derived for the multiphase fields consisting of incompressible Newtonian gas and liquid phases in addition to the visco-hyperelastic phases. The governing equations are given by the following incompressible condition, mass conservation equation and momentum equations respectively:

$$\frac{\partial u_j}{\partial x_j} = 0, \quad \frac{\partial \rho}{\partial t} + \frac{\partial(\rho u_j)}{\partial x_j} = 0 \quad (1)$$

$$\frac{\partial \rho u_i}{\partial t} + \frac{\partial(\rho u_i u_j)}{\partial x_j} = -\frac{\partial p}{\partial x_i} + \frac{\partial(\mu D_{ij})}{\partial x_j} + \frac{\partial(G\phi_s^{1/2} B_{ij}^{*'})}{\partial x_j} + \rho f_i \quad (2)$$

where  $t$  is time,  $x_i$  is the component of Cartesian coordinate system,  $\rho$  is density,  $p$  is pressure,  $\mu$  is the coefficient of viscosity and  $G$  is shear modulus. In addition,  $u_i$  is the velocity component and  $f_i$  is the external force in  $x_i$  direction.  $D_{ij}$  is the component of the deformation rate tensor and  $\phi_s$  is solid volume fraction in a computational cell.  $B_{ij}^{*'}$  is the deviation tensor of  $B_{ij}^*$  which is defined by  $\phi_s^{1/2} B_{ij}^*$ , where  $B_{ij}^*$  is the left Cauchy-Green deformation tensor. The equations of  $\phi_s$  and  $B_{ij}^*$  are given as follows:

$$\frac{\partial \phi_s}{\partial t} + \frac{\partial(\phi_s u_j)}{\partial x_j} = 0, \quad \frac{\partial B_{ij}^*}{\partial t} + \frac{\partial(B_{ij}^* u_k)}{\partial x_k} = L_{ik} B_{kj}^* + B_{ik}^* L_{kj} \quad (3)$$

where  $D_{ij}$ ,  $B_{ij}^{*'}$  and  $L_{ij}$  are given as follows:

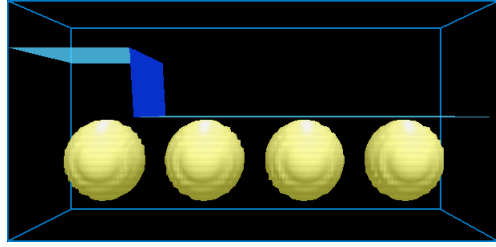
$$D_{ij} = \frac{\partial u_i}{\partial x_j} + \frac{\partial u_j}{\partial x_i}, \quad B_{ij}^{*' } = B_{ij}^* - \frac{1}{3}(\text{tr} B_{ij}^*)\delta_{ij}, \quad L_{ij} = \frac{\partial u_i}{\partial x_j} \quad (4)$$

The governing equations are discretized with FVM on the collocated grid system and they are solved with the modified MAC method [3].

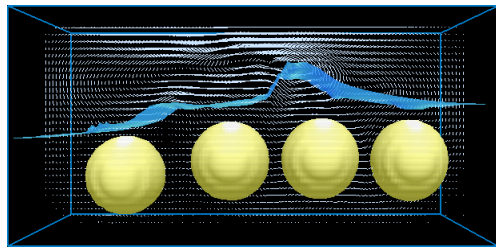
## 3. Results and discussion

As shown in Figs. 1 (a) and 2 (a), showing the same initial conditions of two cases of computations, the present method was applied to dam-break flows including four spherical visco-hyperelastic objects. All variables in computations are non-dimensionalized with representative values. The lengths of the computational volume are 2.1, 1.0 and 1.0 in  $x_1$ ,  $x_2$  and  $x_3$  directions, which correspond to streamwise, transverse and vertical directions, respectively. The gravitational acceleration is  $-10.0$  in  $x_3$  direction. The initial water depths of

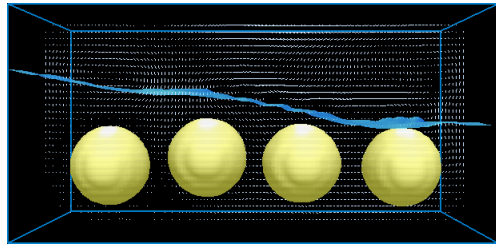
the dam-break condition are 0.8 ( $x_1 \leq 0.25$ ) and 0.5 ( $x_1 > 0.25$ ). The radius of the spherical objects is 0.2 and the interval of the center points of the neighboring two objects is 0.5. The center point of the spherical object on the most left side is located at  $(x_1, x_2, x_3) = (0.3, 0.5, 0.3)$ .



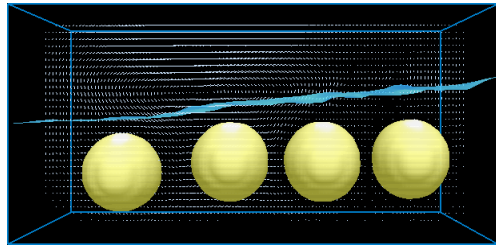
(a)  $t = 0$



(b)  $t = 0.5$

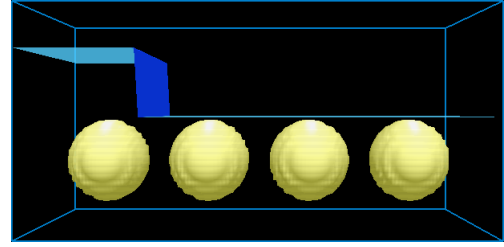


(c)  $t = 1.5$

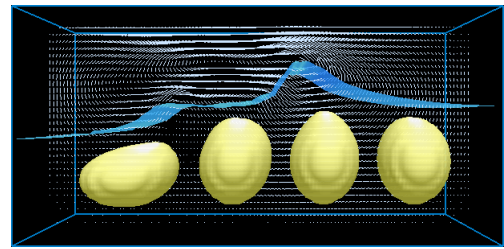


(d)  $t = 2.0$

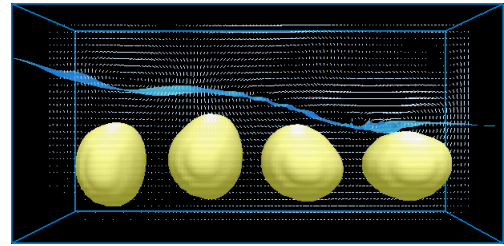
Figure 1: Free surfaces and deformable objects ( $G = 10.0$ )



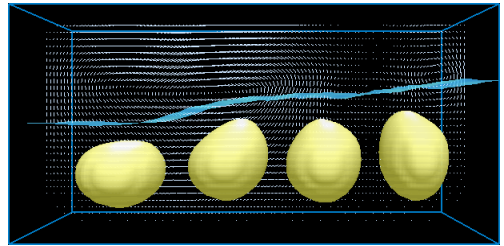
(a)  $t = 0$



(b)  $t = 0.5$



(c)  $t = 1.5$



(d)  $t = 2.0$

Figure 2: Free surfaces and deformable objects ( $G = 0.1$ )

On all boundaries, the pressure boundary conditions  $\partial p / \partial n = 0$  are applied, while non-slip conditions are used for velocity except on the top wall where free-slip condition is adopted. The kinematic viscosity of gas and liquid is set at  $1.0 \times 10^{-2}$ , while the densities of the gas and liquid are 1.0 and  $1.0 \times 10^3$  respectively. The viscous coefficient of the visco-

hyperelastic body is  $1.0 \times 10^{-2}$ , while two cases of computations were conducted with the shear moduli  $G = 10.0$  and  $G = 0.1$  to confirm the damping effects of different  $G$  on the free-surface motions. The density of visco-hyperelastic bodies is  $1.0 \times 10^3$  which is same as that of the liquid phase. Thus, four visco-hyperelastic bodies are suspended in the liquid.

Figure 1 shows the free-surface profiles and the shapes of the four visco-hyperelastic bodies with  $G = 10.0$ , while Fig. 2 shows the results with  $G = 0.1$ . Comparing two results, it can be seen that the visco-hyperelastic bodies are largely deformed due to the interactions with the free-surface flows in case that  $G = 0.1$ .

The time histories of the liquid levels  $h_L$  on the left wall (on the  $x_1 = 0$  section) are shown in Fig. 3. Comparing with the  $h_L$  obtained with no solid bodies, the amplitudes of the liquid levels  $h_L$  are largely decreased when  $G = 10.0$  as shown in Fig. 3 (a), while the damping effects are scarcely found in case of  $G = 0.1$  as indicated in Fig. 3 (b). It can be thought reasonable the effects on the free-surface motions increase as the stiffness of the deformable bodies increases. Conclusively, it can be said that such tendency is successfully demonstrated with the present computational method.

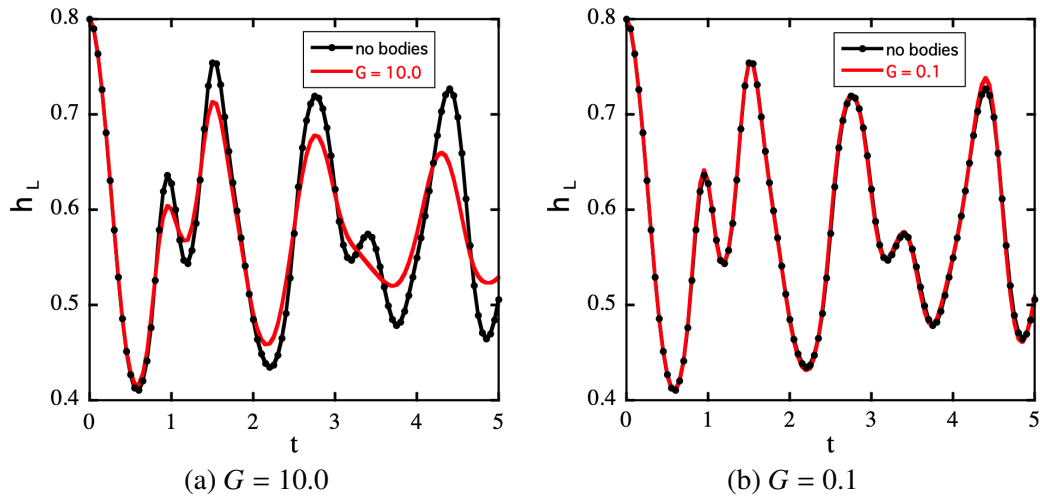


Figure 3: Comparisons of time histories of  $h_L$  with and without objects

## References

- [1] Sugiyama, K., Ii, S., Takeuchi, S., Takagi, S. and Matsumoto, Y.: A full Eulerian finite difference approach for solving fluid-structure coupling problems *Journal of Computational Physics*, Vol. 230, No. 3, pp. 596-627.
- [2] Nishiguchi, K., Maeda, K., Okazawa, S., Tanaka, T.: Euler A Visco-Hyperelastic Analysis Scheme by Using a Full Eulerian Finite Element Method for Dynamics of Pressure-Sensitive Adhesives *Transactions of the Japan Society of Mechanical Engineers, Series A*, Vol. 78 (2012), pp. 375-389.
- [3] Ushijima S., Okuyama Y. and Nezu I.: Implicit computational algorithm for 3D incompressible flows with collocated grid system and its parallelization *J. Applied Mech. JSCE*, Vol. 6 (2003), pp. 185-192.